Volume 1 | Number 1 | Jan 2013 | Pages 1–100

Journal of
Materials Chemistry A

Materials for energy and sustainability
www.rsc.org/materialsA

ROYAL SOCIETY
OF CHEMISTRY

ROYAL SOCIETY
OF CHEMISTRY

www.rsc.org/materialsA

A High Performance Polysiloxane-Based Single Ion Conducting Polymeric Electrolyte Membrane for Applications in Lithium Ion Batteries

Rupesh Rohan,[a], Kapil Pareek,[a] Zhongxin Chen,[a] Weiwei Cai,[a,b] Yunfeng Zhang, [a,b] Guodong Xu,[a] Zhiqiang Gao, [a]Hansong Cheng[a,b]*

[a] Department of Chemistry, National University of Singapore, 3 Science Drive 3, Singapore

 [b] Sustainable Energy Laboratory, Faculty of Materials Science and Chemistry, China University of Geosciences, 388, Lumo Road, Wuhan 430074, P. R. China

ABSTRACT

We report a polysiloxane based single-ion conducting polymer electrolyte (SIPE) synthesized via hydrosilylation technique. Styrenesulfonyl (phenylsulfonyl) imide groups were grafted on the highly flexible polysiloxane chains followed by lithiation. The highly delocalized anionic charges in the grafted moiety give rise to weak association with lithium ions in the polymer matrix, resulting in lithium ion transference number close to unity (0.89) and remarkably high ionic conductivity (7.2 $\times 10^{-4}$ Scm^{-1}) at room temperature. The high flexibility arising from polysiloxane enables the glass transition temperature (T_g) to be below room temperature. The electrolyte membrane displays high thermal stability and a strong mechanical strength. A coin cell assembled with the membrane comprised of the electrolyte and poly(vinylidene-fluoride-co-hexafluoropropene) (PVDF-HFP) performs remarkably well over a wide range of temperature with high charge-discharge rates.

 KEYWORDS: Electrolyte; single ion; hydrosilyaltion; Speier's catalyst; lithium ion battery; transference number.

1. Introduction

Electrolytes play a vital role in battery performance and regulate battery working life. Development of novel electrolytes with high conductivity in a wide temperature range with broad electrochemical window and strong thermal stability is essential for the next generation of lithium-ion battery technologies that utilize high potential electrode materials at high charge-discharge rates. [1-4]

The concept of single ion polymeric electrolyte (SIPE) was proposed with the aim to overcome most of the problems associated with the current electrolytes,[5-22] such as severe concentration polarization and potential safety hazard. Unfortunately, there are also many technical problems with SIPEs. Most notably, these materials exhibit relatively small ionic conductivity and often present high interfacial resistance when used in batteries.[15, 23] To date, few SIPE materials have been demonstrated with satisfactory battery performance. Most SIPEs enable batteries to perform only at elevated temperatures with relatively low charge-discharge rates. [23-29] Indeed, a versatile SIPE capable of sustaining a high C-rate in a wide range of temperature remains to be developed. [30, 31]

It has been well demonstrated that ion migration occurs predominantly in amorphous opulent phase where transport properties, such as ionic conductivity, diffusivity and mechanical relaxation, are explicitly related to the segmental movement of polymers.[30, 32] Therefore, a SIPE with low or no crystallinity and low glass transition temperature with high thermal and electrochemical stability would present a reasonable choice as a battery electrolyte.[31] Unlike most of the polymers used as electrolytes, polysiloxanes, which are inherently amorphous in nature and possess very low Tg with high thermal stability and good mechanical strength, may potentially serve as a useful backbone polymer for designing of SIPEs.[33-35]

Based on this idea, we developed a methodology to synthesize a polysiloxane based single ion conducting gel polymer electrolyte with grafted bis(sulfonyl) imide groups via a hydrosilylation process. Hydrosilylation is a catalyst assisted technique of adding Si-H bonds across unsaturated bonds.[36] In this paper, we describe the synthetic procedure and characterization of this compound. A battery fabricated with the polysiloxane based electrolyte is shown to perform successfully in a temperature range of 25-80 ^{o}C with one of the highest charge-discharge rates reported to date for SIPEs.

2. Experimental

2.1 Materials

Poly(methylhydrogensiloxane) (PMHS) (viscosity-15-40 mPa.S) (Sigma-Aldrich), chloroplatinic acid (Sigma-Aldrich), 4-styrenesulfonic acid, sodium salt (Sigma–Aldrich), oxalyl chloride (Alfa-Aesar), benzenesulfonamide (Sigma–Aldrich), 4-dimethylaminopyrridine (DMAP) (Sigma–Aldrich), triethylamine (Sigma–Aldrich), lithium perchlorate (Sigma–Aldrich), poly(vinylidene fluoride-*co*-hexafluoropropylene) (PVDF-HFP) (Mw- 400,000 gmol^{-1}) (Sigma–Aldrich), 2-propanol (QREC), Acetonitrile (Tedia), dimethylformamide DMF (Sigma–Aldrich), dimethyl sulfoxide (QREC), tetrahydrofuran (THF) (RCI labscan), dichloromethane (QREC). All chemicals were of an analytical grade and used as received.

2.2 Synthesis of potassium 4-styrenesulfonyl (phenylsulfonyl)imide

4-styrenesulfonyl (phenylsulfonyl) imide (SPSIK) was synthesized following the procedure reported by Meziane and co-workers[24, 25] for the synthesis of 4-styrenesulfonyl(trifluoromethylsulfonyl)imide. 40 ml of dried acetonitrile, 0.087 g (1mmol) of DMF along with 2 ml of oxalyl chloride were taken in a two neck flask. The solution was stirred

under argon gas atmosphere at room temperature for 5 hrs to form a Vilsmeier-Haack complex. On completion of the reaction, a light yellow transparent solution was obtained. Subsequently, 4 grams of 4-styrene sulfonic acid sodium salt was added slowly to the solution under argon gas atmosphere and then stirred for 24 hrs. The mixture initially turned yellow and then displayed a light pink color. A NaCl precipitate was separated by filtration and the filtrate (4-styrenesulfonyl chloride) was cooled at 0 $^{\circ}$C.

In a two neck flask, 8.1 ml of triethylamine (58.1 mmol), 3.1 grams of benzenesulfonamide (19.4 mmol) and 2.12 gram of 4-dimethylaminopyrridine (DMAP) were added to 30 ml of dry acetonitrile. The mixture was stirred for 1 hr in argon gas atmosphere and subsequently, the 4-styrenesulfonyl chloride solution cooled at 0 $^{\circ}$C was added slowly to the mixture under stirring for the next 16 hrs. Solvent was removed using a rotavapour and the resultant brown color mass was dissolved in 50 ml of dichloromethane. The solution was washed by a 4% aqueous solution of NaHCO$_3$ (20 ml) twice followed by washing with 20 ml of 1M HCl. The potassium salt of 4-styrenesulfonyl (phenylsulfonyl)imide was obtained by neutralization of the acid moiety in a molar excess aqueous solution of K$_2$CO$_3$. The resulting suspension was stirred at room temperature for 1 hr followed by filtration and drying. The resultant light yellow color solid was further recrystallized in water for 24 hrs at ambient temperature followed by storing in a refrigerator for 12 hrs. The water was decanted and the compound was dried in a vacuum oven at 80 $^{\circ}$C for 12 hrs to obtain dried potassium 4-styrenesulfonyl (phenylsulfonyl)imide with a 50 % yield. Elemental analysis: for C$_{14}$H$_{12}$NO$_4$S$_2$K, calculated: C, 46.52; H, 3.35.; N, 3.87; S, 17.74 %; K, 10.82; found: C, 46.56; H, 3.41; N, 3.61; S, 17.12; K, 10.25. %. ^{1}H NMR (300MHz, DMSO-d$_6$) δ 7.68-7.58 (m, 4 H), 7.49.-7.29 (m, 5 H), 6.73 (dd, J = 17.7, 10.8 Hz, 1 H), 5.87 (d, J = 17.7, 1 H), 5.33 (d, J = 10.8, 1 H)(Fig. S1 in supporting information); ^{13}C NMR (75MHz,

DMSO-d$_6$) δ 146.5, 145.8, 138.6, 135.9, 130.0, 127.8, 126.5, 126.0, 125.5, 115.9 (Fig. S2) .

FTIR data: {ATR(KBr) cm^{-1}}: ν = 3058 (ν$_{CH\ aromatic\ ring}$), 1627 (ν$_{CC\ aromatic\ ring}$), 1445 (β$_{CH\ ring}$ +

ν$_{CCring}$), 1397 (ν$_{asSO2}$), 1300 (β$_{CH}$), 1265 (ν$_{CC}$), 1171 (ν$_{sSO2}$), 1090 (ν$_{CS}$), 1060(ν$_{CC\ ring}$), 840

(ν$_{SN}$), 777(ν$_{SNS}$) and 750 (γ$_{CH}$), 689 (ψ$_{CCC}$), 616 (α$_{CCC}$), {ν: stretching, δ: bending, α and β: in

plane deformation, γ and ψ: out of plane deformation, s: symmetrical, as: asymmetrical}[24, 37-

39], ESI (-) m/z 322.2 (Fig. S6).

2.3 Synthesis of Speier's catalyst

A Speier's catalyst, which conducts hydrosilylation, was synthesized following the procedure

adopted earlier by Chung and Kim.[40] 50 ml of Na dried 2-propanol was taken in a dark color

bottle in which 1 gram of chloroplatinic acid (H$_2$ PtCl$_6$.6H$_2$0) was dissolved. The bottle was kept

for four weeks in a shelf for formation of the Speier's catalyst.

2.4 Synthesis of lithium 4-styrenesulfonyl (phenylsulfonyl)imide grafted poly methyl

hydrogen siloxane (SG) electrolyte

A lithium 4-styrenesulfonyl (phenylsulfonyl)imide grafted poly(methylhydrogensiloxane) (SG)

electrolyte was synthesized via a hydrosilylation reaction in the presence of a Speier's catalyst

(Scheme 1). The SPSIK molecules were grafted onto the poly(methylhydrogen siloxane)

(PMHS) chains, following the method previously reported.[41-43] 0.2 ml of PMHS was mixed

in 10 ml of THF while 1.37 gram of SPSIK was dissolved in 20 ml of DMSO. Both solutions

and 0.1 ml Speier's catalyst were taken in a 2 neck round bottom flask fitted with a magnetic

stirrer and a condenser. To avoid moisture, all operations were performed in a glove box. The

mixture was stirred in argon atmosphere at room temperature for 24 hrs followed by stirring at

80 ^{o}C for another 24 hrs. The completion of hydrosilylation reaction was confirmed by in-situ

FTIR spectrum of the product, in which the sharp and intense peak at 2267 cm^{-1}, corresponding

to the stretch of the Si-H bond, was disappeared. The solvent was removed under vacuum using a freeze-dryer. To remove the unreacted moieties and other impurities, the product was washed with THF, acetone and methanol. Subsequently, the product was dried at 100 ^{o}C for 12 hrs, producing a sticky solid material. To remove the stickiness, the material was heated with acetonitrile at an elevated temperature followed by THF addition upon cooling to retrieve the product. The material was then isolated by filtration and dried at 100 ^{o}C. The process was repeated thrice to obtain a non-sticky light yellow color solid.   Finally, the product was crushed in a fine powder form with mortar and pistol and dried further at 100 ^{o}C in a vacuum oven.

The product was placed in 50 ml of ethanol with stirring and, subsequently, lithium perchlorate (LiClO$_4$) (in excess) was added for the exchange of potassium ions with lithium ions. The solution was heated at 50 ^{o}C for 12 hrs. A white precipitate of potassium perchlorate was filtered out and the solution was removed with a rotary evaporator. The excess of LiClO$_4$ was removed upon solubilization of the solid in DMSO followed by re-precipitation with THF. The final product was dried at 120 ^{o}C under vacuum for 12 hrs. Elemental analysis: for C$_{15}$H$_{16}$NO$_5$S$_2$SiLi, calculated: C, 46.26; H, 4.14.; N, 3.60; S, 16.46; Si, 7.21; Li, 1.78 %; found: C, 46.99; H, 4.49; N, 3.80; S, 17.12; Si, 1.01; Li, 1.61 %. ^{1}H NMR (300MHz, DMSO-d$_6$) δ 7.62-7.08 (m, 9 H), 2.14 (t, J = 8.0 Hz, 2 H), 1.85 (t, J= 7.3 Hz, 2 H), 1.18 (s, 3 H,)(Fig. S3); ^{13}C NMR (75MHz, DMSO-d$_6$) δ 146.5, 145.8, 142.6, 138.9, 136.0, 130.3, 129.2, 128.0, 126.7, 126.3, 125.8, 116.2, 48.8, 30.4, 29.2, 17.4 (Fig. S4) ;   FTIR data: {ATR(KBr) cm^{-1}}: ν = 2978 (ν$_{CH\ alkyl}$), 1648 (ν$_{CC\ aromatic\ ring}$), 1396 (ν$_{asSO2}$), 1267 (δ$_{CH3}$), 1148 (ν$_{sSO2}$), 1091 (ν$_{Si-O-Si}$), 1039 (ν$_{CC\ ring}$) and 778 (ν$_{SNS}$).[39]

2.5 PVDF-HFP/SG membrane preparation

SG and PVDF-HFP were taken in 1:2 proportion and dissolved in 5 ml of a DMF solvent at 60 ^{o}C for 6 hrs in a 50 ml glass beaker fitted with a magnetic stirrer. Subsequently, the mixture was

drop-cast into a teflon petri dish (6 cm diameter) and dried in an oven at 100 $^{\circ}$C to evaporate the DMF solvent. The obtained film was further dried under vacuum at 100 $^{\circ}$C for 24 hrs to remove a trace amount of DMF and then transferred to a glove box. The membrane was punched to obtain a circular film of 1.5 cm diameter. The circular film was subsequently placed in an EC/PC (1:1 volume ratio) solution for soaking and then used for further characterizations and performance assessment in a battery coin cell.
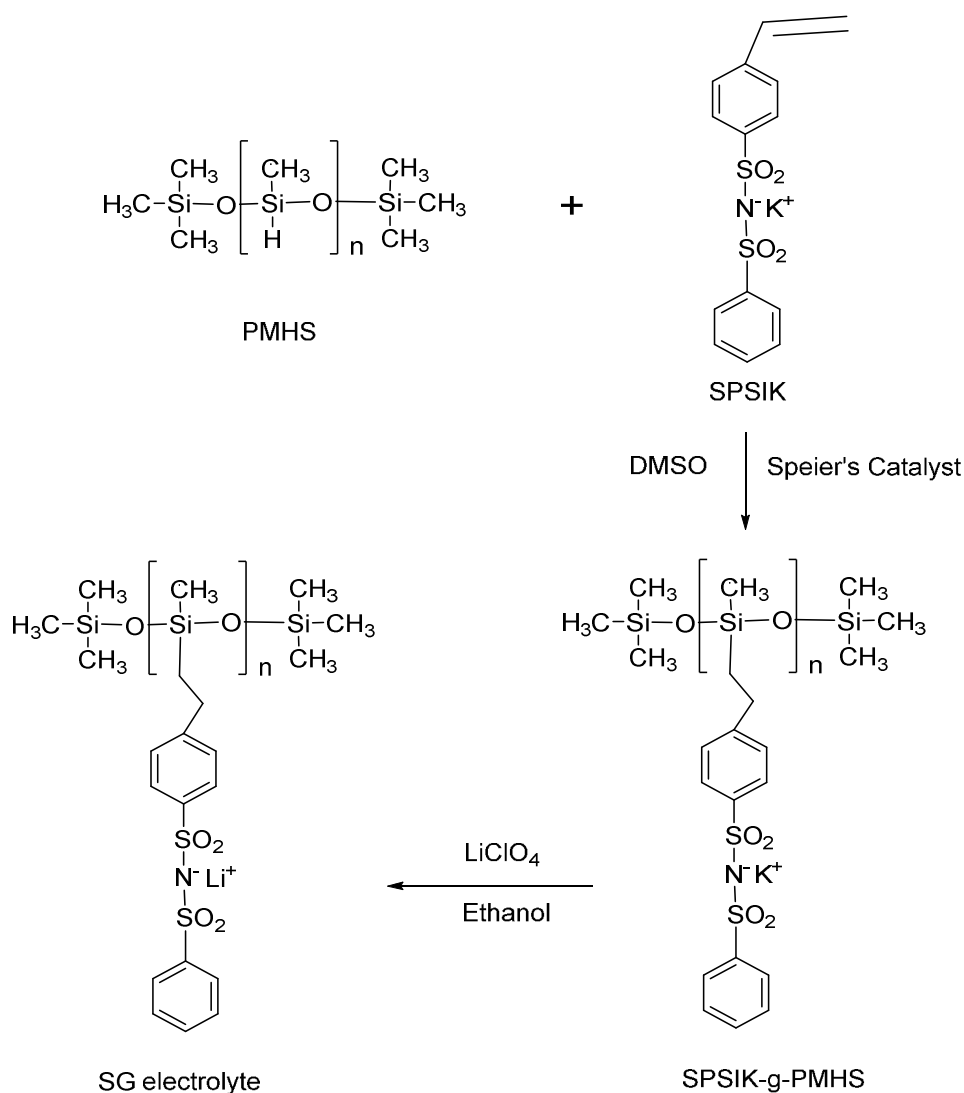
Scheme 1: Synthesis of SG electrolyte.

3. Methods

Gel permeation chromatography (GPC) technique was used for molecular weight and poly dispersity index (PDI) determination. The GPC instrument consists of a high-performance liquid chromatography pump (Waters 515), an autosampler (Waters 2707) and a refractive index detector (Waters 2414). THF was used as an eluent at a flow rate of 0.8 ml/min. A polystyrene standard was used for calibration. All characteristic infrared spectra were recorded in the 400-4000 cm^{-1} frequency range with a Bio-Rad Excalibur FTIR spectrometer. NMR spectra were taken on a Bruker Avance (AV300) spectrometers at 300 MHz, with tetramethylsilane as the standard. Dimethyl sulfoxide-d_6 was used as the solvent for NMR characterization. The microstructures of the samples were determined by using the field emission scanning electron microscopy (FE-SEM) technique on JEOL JSM-6701F Scanning Electron Microscope. Platinum sputtering of the samples was performed under 5×10^{-2} mbar at room temperature (20s, 30mA) prior to the SEM analysis. The thermal gravimetric analysis (TGA) was executed under the N_2 gas inert atmosphere (flow rate: 60 $cm^3 min^{-1}$) at the 10 $^o C min^{-1}$ heating rate from room temperature to 1000 $^o C$ in the Thermo Gravimetric Analyzer (model TGA Q 50) of TA, Inst., USA. Differential Scanning Calorimetry (DSC) study was performed on the DSC-1 (Mettler Tolledo, Inst., USA) instrument in N_2 atmosphere (flow rate: 60 $cm^3 min^{-1}$) from -60 $^o C$ to 150 $^o C$ with the heating rate of 10 $^o C min^{-1}$.

Elemental analysis for C, H, N and S elements determination was performed using a CHNS analyser, model Vario Microcube from Elementar Analysensysteme. Samples were weighed (1-2mg) in a tin capsule and combusted at 1150°C. The combustion products such as CO_2, SO_2, NO_2 are carried by Helium carrier gas into the reduction tube containing copper where NO_2 is

converted to N_2 and any unconsumed oxygen is removed. N_2 passes through to be detected by the conductivity detector. The rest of the gases are retained on the adsorption column. The desorption column is heated to release each of the gases at different temperatures which are detected by thermal conductivity detector. Calibration is performed using high purity sulfanilamide. Metals content was determined by acid digestion of the samples followed by analyses with the Inductively Coupled Plasma Optical Emission Spectrometer (ICP-OES), model Optima 5300DV from Perkin Elmer. Multi element standards from Inorganic Venture were used for calibration.

The ionic conductivity of the electrolyte membrane was calculated by electrochemical impedance spectroscopy (EIS) using the Zahner potentiostate-galvanostatate electrochemical workstation (model PGSTAT) over a frequency range of 4×10^6 to 1 Hz with an oscillating voltage of 5 mV. The electrolyte membrane was placed in a stainless steel cylindrical device of 1.5 cm diameter sealed in a glove box under argon atmosphere. Before the EIS analysis, the device was heated at 80 ^{o}C to enhance the contact between the surfaces of the device plates serving as the electrodes and the electrolytic membrane. The Simulated Impedance Measurement (SIM) software was used for fitting of the EIS data.

The transference number of the electrolyte was calculated by the method proposed by Evans and co-workers, based on the combination of DC and AC electrical polarizations as.[44] The value of cationic transference number (t_{Li}^+) was calculated according to the following equation:

$$t_{Li}^+ = \frac{I_s\left(\Delta V - I_o R_o\right)}{I_o\left(\Delta V - I_s R_s\right)}$$

where ΔV is the DC potential applied across the cell; I_s and I_o are the steady-state and the initial current determined by the DC polarization, respectively. R_o and R_s are the EIS measured bulk resistances before and after the DC polarization

To measure the battery performance, a multichannel battery testing instrument, Arbin BT-2000, was used. The charge and discharge capacity of the coin cells assembled with the electrolyte membrane was measured with different C-rates at various temperatures. The composite cathode consists of $LiFePO_4$ (75%), PVDF (10%), acetylene black (10%) and a small amount of lithium bis(4-carboxy phenyl sulfonyl)imide (5%) as a supporting electrolyte. All the ingredients were mixed and well stirred in a NMP solvent. The prepared ink was then cast onto an aluminum foil and subsequently dried in a vacuum oven at 80 ^{o}C for 12 hrs. The dried cathode was then cut into a circular shape for use in coin cells. The coin cells assembly was performed inside a glove box. For coin cell assembly, stainless-steel cup and lids of coin cells CR 2025 (20 mm diameter 2.5 mm thickness) comprised with $LiFePO_4$ cathode, Li metal anode and EC/PC swollen single ion polymer electrolyte membrane were used. The cathode was placed in the centre of the cup which forms +ve terminal of the cell and subsequently covered with the swollen polymer electrolyte membrane. Circular lithium metal disc of 13 mm diameter and ~0.6 mm thickness was placed centrally upon the membrane. To ensure good sealing and achieve proper thickness of the materials, two stainless discs (spacers) followed by a steel spring, which formed −ve terminal, were fixed upon the Li metal disc. Finally, the coin cell was closed with the lid and final sealing was done with automatic coin crimper machine. The assembled cells were then transferred outside the glove box and aged/equilibrated for 12 prior to further electrochemical characterizations.

4. Results and discussion

4.1 Synthesis and characterization of potassium 4-styrenesulfonyl(phenylsulfonyl)imide (SPSIK)

The SPSIK monomer was synthesized following the method proposed by Meziane et al. with a slight difference in choice of one of the ingredients.[24, 25] In this work, benzene sulfonamide was used in place of trifluoromethylsulfonamide (TFSI), which was used in the original method. The rest of ingredients including catalyst and solvents as well as the synthetic route were kept the same. Successful synthesis of SPSIK was confirmed by ^{1}H NMR, elemental analysis and mass spectroscopy (ESI-HRMS). The ^{1}H NMR signals corresponding to 12 H atoms (9 aromatic and 3 non-aromatic) with the peak area ratio of 9:1:1:1 further confirms the target structure. Moreover, the molecular formula of SPSIK calculated in negative mode of ESI-HRMS was found to be 322.2, which matches well with the theoretical value of 322.3 for the anion monomer $C_{14}H_{12}NO_4S_2$. Finally, the agreement between the expected and the found values of elemental analysis data reaffirms the successful synthesis of SPSIK.

4.2 Synthesis and characterization of lithium 4-styrenesulfonyl (phenylsulfonyl)imide grafted poly methyl hydrogen siloxane (SG) electrolyte and PVDF-HFP/SG blend membrane

The SG electrolyte was synthesized by grafting SPSIK on polymethyl hydrogen siloxane (PMHS) chains (SPSIK-g-PMHS) via hyrdosilylation followed by lithium ion exchange. Hydrosilylation is the most versatile platinum catalyst assisted technique used for addition of Si-H on unsaturated bonds.[36, 45] The Speier's catalyst (solution of chloroplatinic acid in 2-proponal) facilitates the addition of unsaturated groups on Si-H according to anti-Markovnikov's

rule in a three step cyclic process.[36] Following the same mechanism, here, the vinylic part of SPSIK was attached to the polysiloxane chains upon addition of a Si-H bond.

The grafting of SPSIK on PMHS chains followed by exchange of K^+ ions by Li^+ ions was clearly proven to be successful by FTIR and NMR spectra. As can be seen in the FTIR spectra of PMHS and SG (Fig. 1), the peak at 2167 cm^{-1} in PMHS, corresponding to Si-H bond, is disappeared in SG, which confirms the grafting of SPSIK. In addition, the peak at 1627 cm^{-1} in SPSIK, corresponding to the vinylic group, is also disappeared in SG, confirming the grafting, which consumes the vinylic group. Furthermore, the signature signal of Si-H, appears at 4.68 ppm (^{1}H NMR) in PMHS, and the three peaks in the range of 6.78 to 5.31 ppm (^{1}H NMR) in SPSIK corresponding to 3 vinylic protons, are disappeared in SG, validating the grafting of SP on the PMHS chains.[43, 46]. Finally, the overall synthesis of SG electrolyte was confirmed by the coherence between the expected and the found values for all the elements, except for Si, in the elemental analysis. The deviation observed for Si is mainly attributed to the incomplete digestion of Si during the analysis, which was also noticed during the elemental analysis of commercial products of Si such as PMHS and poly(methylphenylsiloxane)(PMPS) (Table S1 in Supporting Information). The GPC analysis of SG in the tetrahydrofuran (THF) mobile phase depicts the number average molecular weight (Mn) of 84,238, weight average molecular weight (Mw) of 150,230, and poly dispersity index (PDI) of 1.78 based on the polystyrene standard.
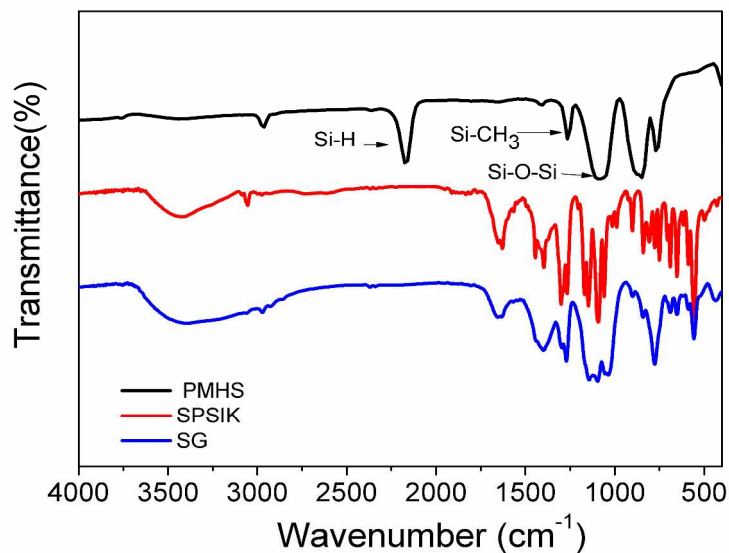
Figure 1: The FTIR spectra of PMHS, SPSIK and SG electrolyte.

Since it was not possible to form a free standing membrane of SG electrolyte alone, PVDF-HFP was used as a binder. The reason for choosing PVDF-HFP was based on the following considerations. Although poly ethylene oxide (PEO) is one of the most extensively utilized binders for polymer electrolytes, it may cause severe passivation upon contact with a lithium metal anode. On the other hand, PVDF, a homo polymer, exhibits strong electrochemical stability arising from the strong electron withdrawing fluorine atoms in the compound. It has a high dieletric constant of 8.4, which helps in greater ionization of lithium salts. However, due to its crystalline nature, PVDF may cause separation of solvent liquids from the membrane surface (knowns as syneresis), which may result in a leakage of a solvent and thus become a safety hazard when used in batteries. As the advanced version of a PVDF based polymer, PVDF-HFP, the copolymer of vinylidene fluoride and hexafluoropropylene, performs better than PVDF mainly due to the presence of an amorphous domain of hexafluoro propylene, which overcomes the problem of syneresis. [47]

Figure 2 depicts the thermal degradation of the SG electrolyte and SG/PVDF-HFP membrane, in N$_2$ gas atmosphere. For SG electrolyte, after the 5% initial weight loss till 180 ^{o}C, which is attributed to the loss of moisture and a trace amount of the solvents, no degradation occurs till 410 ^{o}C. A two stage of degradation starts after 410 ^{o}C and ultimately diminishes at 1000 ^{o}C with ca. 10% of char. The results confirm the high thermal stability of the SG electrolyte at an elevated temperature, which is a typical feature of polysiloxanes. The residual weight of the sample, on completion of the TGA analysis, corresponds to the total Si and Li contents of the material. For SG/PVDF-HFP membrane, the TGA thermogram shows stability up to 450 ^{o}C before showing a single step degradation. The high thermal stability of the membrane is mainly attributed to the thermal stability of both SG electrolyte and PVDF-HFP (degradation temperature > 460 ^{o}C).[48] The TGA suggests that the SG electrolyte and the SG/PVDF-HFP membrane should also be potentially useful for high temperature applications of batteries.
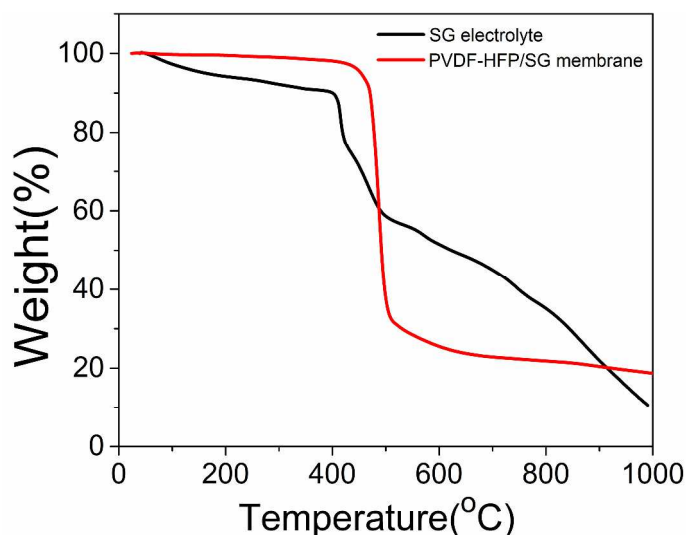

Figure 2. The TGA thermogram of SG electrolyte and PVDF-HFP/SG membrane (N$_2$, 10 ^{o}C min^{-1}, RT to 1000 ^{o}C).

The DSC thermograms of the SG electrolyte and SG/PVDF-HFP membrane are shown in Fig. 3. The glass transition temperature (T$_g$) of SG was found to be 10 ^{o}C, fairly below the room

temperature and the lowest among the SIPEs reported to date.[23, 24, 27, 49, 50] The low T_g arises mainly due to PMHS, the parent polysiloxane chain. Polysiloxane is known for its very low glass transition temperature (~ -100 ^{o}C) due to the presence of highly flexible Si-O-Si bonds. This is the main reason for PMHS was selected as the base polymer. The grafting of bulky SPSIK group on PMHS increases the T_g of the resultant SG electrolyte; however, the T_g still remains well below the room temperature. The absence of a melting peak below 150 ^{o}C, which was expected due to the inherent amorphous nature of PMHS, confirms the amorphous nature of the SG electrolyte. The low temperature flexibility of SG electrolyte as well as of PVDF-HFP (Tg ~ -35 ^{o}C) works synergistically for the SG/PVDF-HFP membrane and as a result, the T_g of the membrane was found to be -17 ^{o}C, which ensures high flexibility of the membrane and consequently, a decent performance of the membrane .[51] Furthermore, the low crystallinity of the membrane coupled with low T_g makes the membrane well suited as a single ion conducting electrolyte membrane for lithium ion batteries.
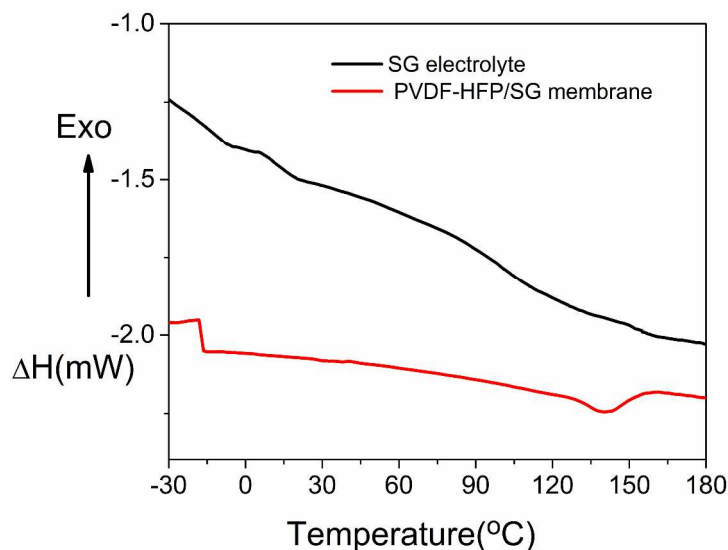

Figure 3. The DSC thermogram of SG electrolyte and PVDF-HFP/SG membrane (N$_2$, 10 ^{o}C min^{-1}, -30 to 180 ^{o}C).

The SEM image of the SG electrolyte is shown in Fig. 4a. The powder forms irregularly shaped aggregates, which is attributed to the high polarization of the particles in view of the presence of high polar groups. The morphology of the PVDF-HFP/SG blend membrane is depicted in its SEM images (Figs. 4b and 4c). There are some blind pores found on the surface of the membrane (Fig.4b). However, from the cross section of the membrane (Fig.4c), no pores are visible, indicating the dense nature of the membrane. The blind pores may be formed due to the evaporation of the solvent from the surface. The tensile strength of the membrane was found to be 5.8 MPa with elongation at break of 18% (Fig. 4d), inferring its sufficiently high mechanical strength. The membrane plays a dual role as a separator and as an electrolyte for battery operation. To assess the mechanical strength of the membrane further, it was clamped between two clips against the gravity and a 15 gram stainless steel cylinder was kept upon the membrane (Fig. 4e). The membrane withstood the load of the cylinder successfully without showing a sign of mechanical failure, which confirms its suitability as an electrolyte membrane for battery assembly. In addition, the membrane displays high flexibility (Fig. 4f), which enables significant reduction of interfacial resistance between electrodes and the membrane and thus enhances battery performance.
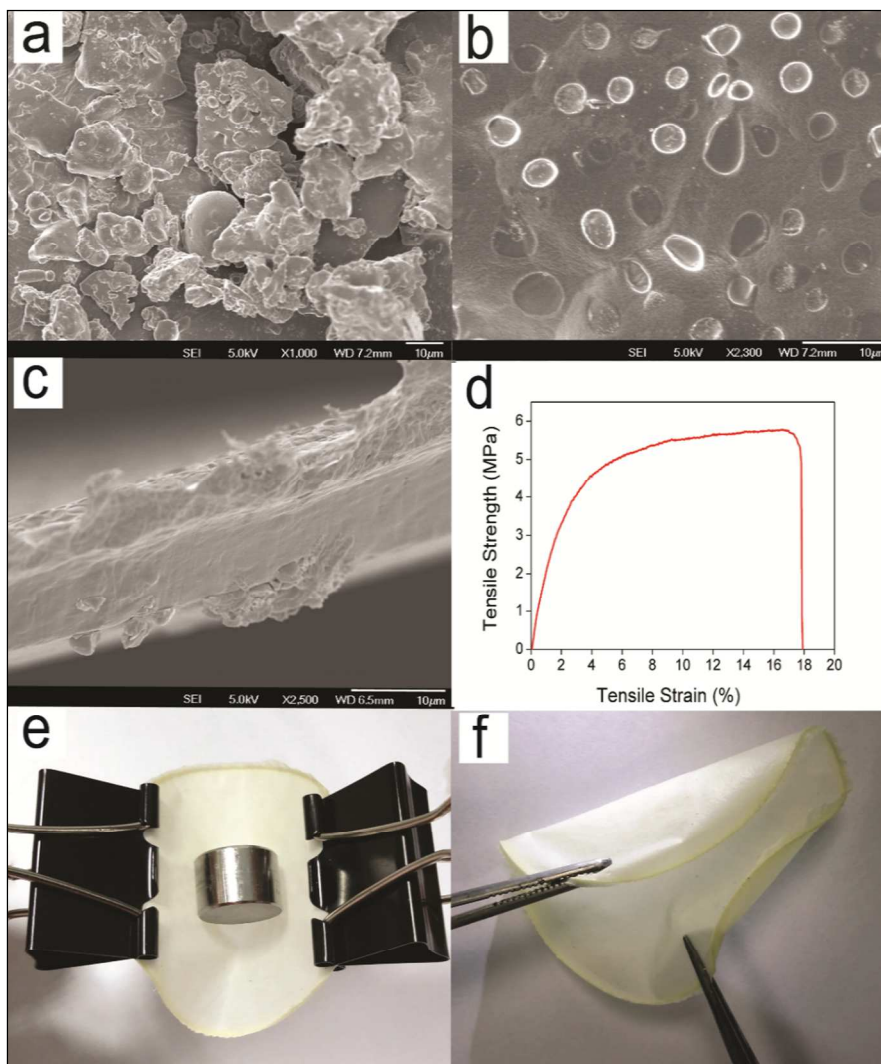
Figure 4. **(a) SEM image of SG electrolyte, (b) SEM image of surface view of PVDF-HFP/SG membrane, (c) SEM image of cross-sectional view of PVDF-HFP/SG membrane (d) tensile strength vs tensile strain graph of PVDF-HFP/SG membrane, (e) photograph of clamped PVDF-HFP/SG membrane holding a stainless steel cylinder of 15 gram weight, (f) photograph of flexible nature of PVDF-HFP/SG membrane.**

4.3 Electrochemical Properties

The Electrochemical Impedance Spectroscopy (EIS) response of the PVDF-HFP/SG (soaked in

an EC/PC solution) was recorded at different temperatures and the results are plotted in Nyquist

coordinates (Z' Vs Z''), where Z' and Z'' are the real and imaginary parts of the impedance,

respectively (Fig. 5). The equivalent circuit used for the fitting is also depicted in the inset of the Fig. 5, where R1, R2, CPE and W stand for the bulk resistance, the interface resistance, the constant phase element and the Warburg resistance, respectively.
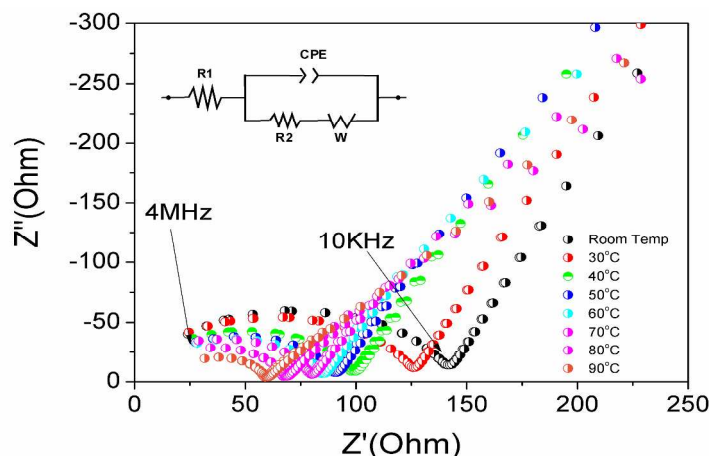

Figure 5. The EIS plot of the PVDF-HFP/SG membrane at various temperatures. The inset is the corresponding equivalent circuit.

The ionic conductivity of the membrane at different temperatures was derived based on the fitting results of the EIS responses obtained at the given temperatures.[27] At room temperature, the ionic conductivity of the membrane was calculated to be 7.2×10^{-4} Scm^{-1}, which is slightly higher than the conductivity displayed by most single ion gel polymeric electrolytes reported to date.[6, 8, 26, 52, 53] The high conductivity of the electrolyte mainly arises from the electrons delocalization of the N atom of the bisulfonyl imide group via the strong electron withdrawing functionality of the adjacent S=O groups. The electron delocalization is further enhanced in the presence of the two benzene rings at both ends. The delocalization thus gives rise to weak association between cations and anions. The charge separation in the membrane enables high Li ion mobility, which is further supported by the high flexibility of the main chains with Si-O-Si bonds.

To analyze the temperature-dependency of the ionic conductivity of the PVDF-HFP/SG membrane, a graph is plotted between the log values of the ionic conductivity of the membrane vs. the inverse of absolute temperatures (Fig 6), for the testing temperature range from 90 ^{o}C to room temperature downwards. As expected, the measured log value of the ionic conductivity increases linearly with temperature, exhibiting coherence with a typical Arrhenius curve but not as steep as in what was observed with dual-ion based small molecular gel polymer electrolytes.[54, 55] The meek increment in the ionic conductivity may be attributed to the mechanical coupling between ion transport and polymer host mobility at a given temperature according to the free volume law.[7] The highest conductivity at 90 ^{o}C was found to be 1.13 ×10^{-3} Scm^{-1}.
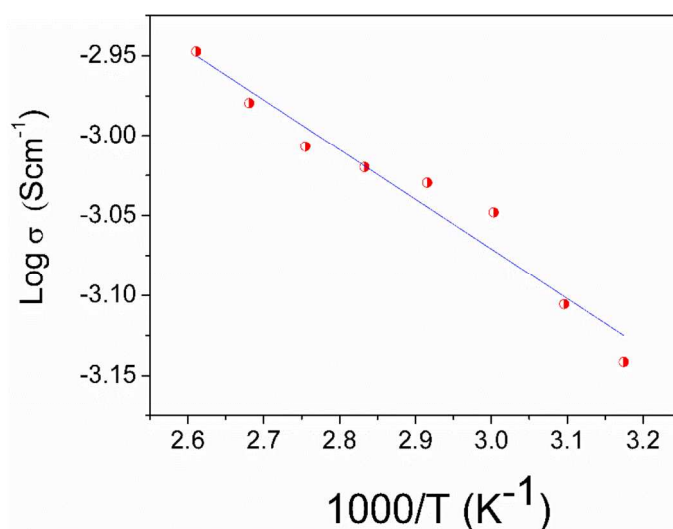

Figure 6.   The Arrhenius plot of log (ionic conductivity) versus inverse absolute temperature.

To calculate the lithium-ion transference number (t_{Li}^{+}), Li│PVDF-HFP/SG membrane │Li cell was assembled, where the membrane was slotted in between two non-blocking lithium metal electrodes.[25, 56] The value of variables required for the calculation are depicted in the Table 1.

The t_{Li}^+ value was calculated to be 0.89 at room temperature, which infers the single-ion conducting behaviour of the SG electrolyte as presumed.

Table 1. Parameters for calculation of lithium ion transference numbers (t_{Li}^+).

ΔV	$I_0\,(\mu A)$	$I_S\,(\mu A)$	$R_0\,(\Omega)$	$R_S\,(\Omega)$	$t^+ = \dfrac{I_S(\Delta V - I_0 R_0)}{I_0(\Delta V - I_S R_S)}$
0.01	8.68	7.72	49.30	50.35	0.89

To evaluate the electrochemical stability of the PVDF-HFP/SG membrane, cyclic voltammetry (CV) study was carried out using the Li│PVDF-HFP/SG membrane│stainless-steel cell. The CV was performed at room temperature between 0 and 6V (versus Li^+/Li) at a scan rate of 1 mV/s and the response is plotted as a current vs voltage curve, as depicted in Fig 7. There is no significant fluctuation observed in the current below 4.1V at room temperature, which infers the electrochemical suitability of the SG/PVDF-HFP membrane with the most available cathode materials.
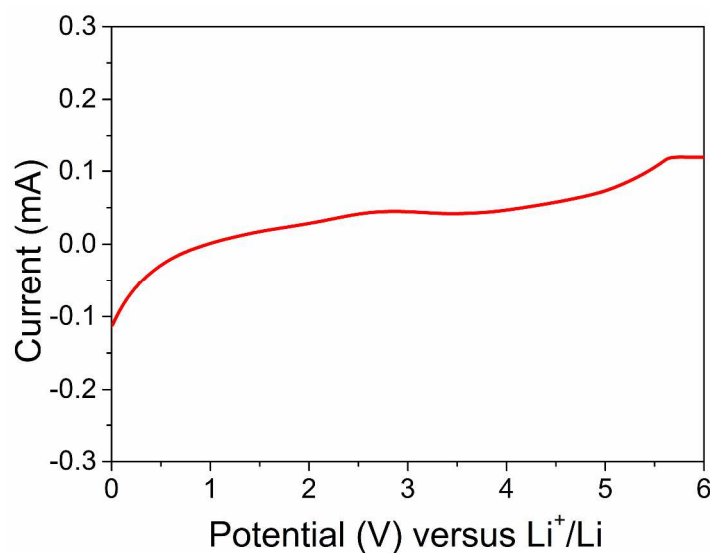

Figure 7. Cyclic Voltammetry of PVDF-HFP/SG membrane at room temperature with the scan rate of 1mV/s. (cathodic part only).

The galvanostatic charge-discharge cyclic performance of the PVDF-HFP/SG membrane was investigated in the voltage window of 2.4-3.8 V at various C-rates. The PVDF-HFP/SG membrane was sandwiched between a lithium metal anode and a $LiFePO_4$ composite cathode (theoretical discharge capacity: 170 mAhg^{-1}) in a coin cell.[57] Figure 8 displays the characteristic evolution of the battery voltage of the cell Li│PVDF-HFP/SG membrane (EC/PC)│ $LiFePO_4$ as a function of its discharge capacity at room temperature, 60 °C and 80 °C, respectively. The discharge curves exhibit a typical three step plateau profile of the $LiFePO_4$ cathode material with the initial discharge capacities of 141, 159 and 154 mAhg^{-1} at room temperature, 60 °C and 80 °C, respectively, at 0.1 C rate.[23, 29, 52] Correspondingly, the initial coulombic efficiencies were found to be 87, 88 and 93%. The slight increment of the plateau voltage at the elevated temperatures may be attributed to the presence of the extra Li ions at the cathode-PVDF-HFP/SG interface. The high Li mobility in the electrolyte membrane enables Li ions to be released more readily at an elevated temperature. The ions are collected at the interface and offer some extra resistance. As a consequent, the voltage increases.[58]
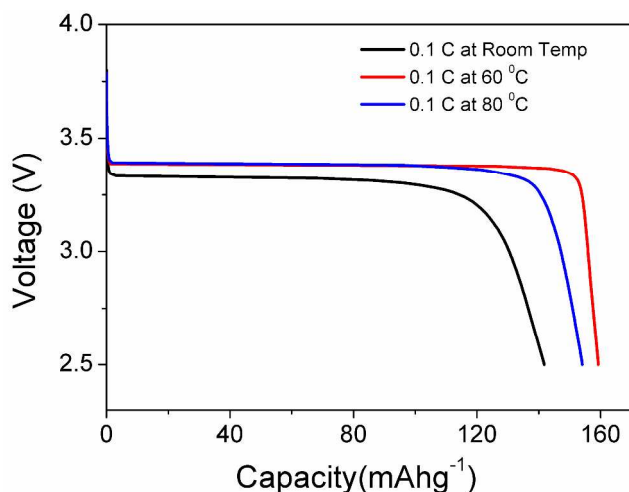

Figure 8. The discharge profiles of Li│PVDF-HFP/SG membrane (EC/PC)│ $LiFePO_4$ battery coin cell obtained at room temperature, 60 °C and 80 °C for 0.1C rate

The discharge capacity vs. cycle number of the cell is depicted in Fig. 9. The discharge capacity of the cell at room temperature was found to be 141 mAhg^{-1} at 0.1C and 135 mAhg^{-1} at 0.2 C. In particular, the battery performs very well at 60 $^{\mathrm{o}}$C with a C-rate up to 3C. At this temperature, the discharge capacity was found to be near 160 mAhg^{-1} for low C-rates and decrease gradually as the rate increases. However, the capacity still remains above 110 mAhg^{-1} at 2 C. The battery also performs very well on 80 $^{\mathrm{o}}$C up to 2 C but becomes slightly inferior than at 60 $^{\mathrm{o}}$C, which may be due to the reduction of electrochemical stability at the elevated temperature. The reason for the good battery performance is attributed to (i) the low T$_{\mathrm{g}}$ of the electrolyte which makes the membrane more flexible, reduces the interfacial resistance between the electrodes and the electrolyte and supports facile transport of Li ions, and (ii) the high lithium transference number, which limits the concentration polarization effect .[59]
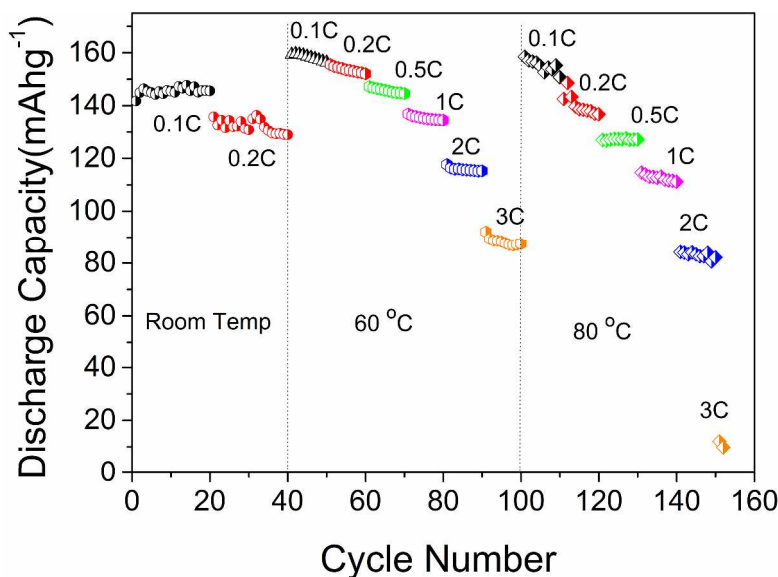

Figure 9. The discharge capacity vs. cycle index of the Li│PVDF-HFP/ SG membrane (EC/PC)│ LiFePO$_4$ battery coin cell obtained at room temperature, 60 $^{\mathrm{o}}$C and 80 $^{\mathrm{o}}$C at various C-rates.

Summary

A novel approach of synthesizing a new class of single-ion polymer electrolytes based on a polysiloxane polymer and a hydrosilylation technique is demonstrated in the present work. Lithium styrenesulfonyl (phenylsulfonyl) imide grafted polymethyl hydrogen siloxane (SG) electrolyte was successfully synthesized. The chemical structures and properties of the electrolyte and its composite membrane with PVDF-HFP were thoroughly characterized via a range of spectroscopic techniques including FTIR, NMR, TGA, DSC analysis, EIS and CV. The highly flexible nature of SG electrolyte (Tg 10 $^{\circ}$C) enables significant reduction of interfacial resistance between the electrodes and the electrolyte membrane. As a consequence, the battery cell incorporated with the electrolyte membrane performs very well in a wide range of temperatures. The polymer electrolyte exhibits good thermal stability up to 410 $^{\circ}$C and electrochemical stability up to 4.1 V with remarkably high ionic conductivity of 7.2×10^{-4} Scm^{-1} at room temperature. The high ion conduction is attributed to the extensive electron delocalization through the bis sulfonyl imide groups, leading to significant enhancement of mobility of lithium ions. The measured lithium ion transference number is close to unity (0.89), substantially higher than the value of typical dual-ion based electrolytes. The reasonably wide electrochemical window enables the electrolyte membrane to be potentially useful for batteries with a range of cathode materials. Furthermore, the battery performance of the SIPE membrane was evaluated with an assembled coin cell of Li│PVDF-HFP/SG membrane (EC/PC)│ LiFePO$_4$. The battery displays high charge and discharge rates with good columbic efficiency at elevated temperatures. The successful demonstration of the electrolyte membrane may pave the way to develop new SIPEs with high flexibility at low temperature, high ionic conductivity, and high thermal and electrochemical stability. Finally, the applied synthetic route may serve as a

useful protocol for grafting desired ionic conductive moieties in Si-H containing polymers with

tailored properties.

Acknowledgments

Corresponding Author Address
*chghs2@gmail.com

References

1.   Cheng, F., et al., *Functional materials for rechargeable batteries.* Advanced Materials, 2011. **23**(15): p. 1695-1715.
2.   Bruce, P.G., et al., *Li-O2 and Li-S batteries with high energy storage.* Nat Mater, 2012. **11**(1): p. 19-29.
3.   Bruce, P.G., B. Scrosati, and J.-M. Tarascon, *Nanomaterials for Rechargeable Lithium Batteries.* Angewandte Chemie International Edition, 2008. **47**(16): p. 2930-2946.
4.   Tarascon, J.M. and M. Armand, *Issues and challenges facing rechargeable lithium batteries.* Nature, 2001. **414**(6861): p. 359-367.
5.   Mandal, B.K., et al., *New Class of Single-Ion-Conducting Solid Polymer Electrolytes Derived from Polyphenols.* Chemistry of Materials, 2000. **12**(1): p. 6-8.
6.   Watanabe, M., Y. Suzuki, and A. Nishimoto, *Single ion conduction in polyether electrolytes alloyed with lithium salt of a perfluorinated polyimide.* Electrochimica Acta, 2000. **45**(8–9): p. 1187-1192.
7.   Geiculescu, O.E., et al., *Solid polymer electrolytes from polyanionic lithium salts based on the LiTFSI anion structure.* Journal of The Electrochemical Society, 2004. **151**(9): p. A1363-A1368.
8.   Tian, L.-Y., X.-B. Huang, and X.-Z. Tang, *Single-ionic gel polymer electrolyte based on polyvinylidene fluoride and fluorine-containing ionomer.* European Polymer Journal, 2004. **40**(4): p. 735-742.
9.   Sun, X.-G., C.L. Reeder, and J.B. Kerr, *Synthesis and characterization of network type single ion conductors.* Macromolecules, 2004. **37**(6): p. 2219-2227.
10.   Dou, S.C., et al., *Synthesis and characterization of poly(ethylene glycol)-based single-ion conductors.* Chemistry of Materials, 2006. **18**(18): p. 4288-4295.
11.   Matsumi, N., et al., *Polymerized Ionic Liquids via Hydroboration Polymerization as Single Ion Conductive Polymer Electrolytes.* Macromolecules, 2006. **39**(20): p. 6924-6927.
12.   Cakmak, G., A. Verhoeven, and M. Jansen, *Synthesis and characterization of solid single ion conductors based on poly[lithium tetrakis(ethyleneboryl)borate].* Journal of Materials Chemistry, 2009. **19**(25): p. 4310-4318.

13.   Itoh, T., et al., *Solid polymer electrolytes composed of polyanionic lithium salts and polyethers.* Journal of Power Sources, 2009. **189**(1): p. 531-535.

14.   Rohan, R., et al., *Melamine-Terephthalaldehyde-Lithium Complex: A Porous Organic Network Based Single Ion Electrolyte for Lithium Ion Batteries.* Journal of Materials Chemistry A, 2015. **3**: p. 5132-5139.

15.   Xu, G., et al., *A lithium poly(pyromellitic acid borate) gel electrolyte membrane for lithium-ion batteries.* Journal of Materials Science, 2014. **49**(17): p. 6111-6117.

16.   Xu, G., et al., *Synthesis, Characterization and Battery Performance of A Lithium Poly (4-vinylphenol) Phenolate Borate Composite Membrane.* Electrochimica Acta, 2014. **139**(0): p. 264-269.

17.   Zhang, Y., et al., *Design and synthesis of a single ion conducting block copolymer electrolyte with multifunctionality for lithium ion batteries.* RSC Advances, 2014. **4**(83): p. 43857-43864.

18.   Zhang, Y., et al., *Influence of Chemical Microstructure of Single-Ion Polymeric Electrolyte Membranes on Performance of Lithium-Ion Batteries.* ACS Applied Materials & Interfaces, 2014. **6**(20): p. 17534-17542.

19.   Zhang, Y., et al., *A gel single ion polymer electrolyte membrane for lithium-ion batteries with wide-temperature range operability.* RSC Advances, 2014. **4**(40): p. 21163-21170.

20.   Zhang, Y., et al., *Lithium-Ion Batteries with a Wide Temperature Range Operability Enabled by Highly Conductive sp3 Boron-Based Single Ion Polymer Electrolytes.* Energy Technology, 2014. **2**(7): p. 643-650.

21.   Zhang, Y., et al., *A class of sp3 boron-based single-ion polymeric electrolytes for lithium ion batteries.* RSC Advances, 2013. **3**(35): p. 14934-14937.

22.   Xu, G., et al., *A novel sp3Al-based porous single-ion polymer electrolyte for lithium ion batteries.* RSC Advances, 2015. **5**: p. 32343-32349.

23.   Bouchet, R., et al., *Single-ion BAB triblock copolymers as highly efficient electrolytes for lithium-metal batteries.* Nat Mater, 2013. **12**(5): p. 452-457.

24.   Meziane, R., et al., *Single-ion polymer electrolytes based on a delocalized polyanion for lithium batteries.* Electrochimica Acta, 2011. **57**(0): p. 14-19.

25.   Feng, S., et al., *Single lithium-ion conducting polymer electrolytes based on poly[(4-styrenesulfonyl)(trifluoromethanesulfonyl)imide] anions.* Electrochimica Acta, 2013. **93**(0): p. 254-263.

26.   Zhu, Y.S., et al., *A new single-ion polymer electrolyte based on polyvinyl alcohol for lithium ion batteries.* Electrochimica Acta, 2013. **87**(0): p. 113-118.

27.   Rohan, R., et al., *Functionalized meso/macro-porous single ion polymeric electrolyte for applications in lithium ion batteries.* Journal of Materials Chemistry A, 2014. **2**(9): p. 2960-2967.

28.   Soo Lee, A.S., et al., *Novel polysilsesquioxane hybrid polymer electrolytes for lithium ion batteries.* Journal of Materials Chemistry A, 2014. **2**(5): p. 1277-1283.

29.   Wang, X., et al., *Exploring polymeric lithium tartaric acid borate for thermally resistant polymer electrolyte of lithium batteries.* Electrochimica Acta, 2013. **92**(0): p. 132-138.

30.   Money, B.K., K. Hariharan, and J. Swenson, *Glass Transition and Relaxation Processes of Nanocomposite Polymer Electrolytes.* The Journal of Physical Chemistry B, 2012. **116**(26): p. 7762-7770.

31.   Kerr, J.B., *Polymeric Electrolytes: An Overview*, in *Lithium Batteries*, G.-A. Nazri and G. Pistoia, Editors. 2003, Springer US. p. 575-622.

32.   Wintersgill, M.C. and J.J. Fontanella, *Polymer Electrolyte Reviews 2*, J.R. MacCallum and C.A. Vincent, Editors. 1989, Elsevier : London, New York. p. 43.

33.   Mark, J.E., *Some Interesting Things about Polysiloxanes.* Accounts of Chemical Research, 2004. **37**(12): p. 946-953.

34. Moretto, H.-H., M. Schulze, and G. Wagner, *Silicones*, in *Ullmann's Encyclopedia of Industrial Chemistry*. 2000, Wiley-VCH Verlag GmbH & Co. KGaA.

35. Pareek, K., et al., *Synthesis, Characterization and Properties of New Fluorinated Poly(imide siloxane) Co-polymers from 4,4′-(Hexafluoro-isopropylidene)diphthalic Anhydride.* Designed Monomers and Polymers, 2010. **13**(3): p. 221-236.

36. Marciniec, B., *Hydrosilylation of Alkenes and Their Derivatives*, in *Hydrosilylation*, B. Marciniec, Editor. 2009, Springer Netherlands. p. 3-51.

37. Tanaka, Y. and Y. Tanaka, *Infrared spectra of bisaryl sulphonimide derivatives.* Chemical & Pharmaceutical Bulletin, 1974. **22**: p. 2546-2551.

38. Lassègues, J.-C., et al., *Spectroscopic Identification of the Lithium Ion Transporting Species in LiTFSI-Doped Ionic Liquids.* The Journal of Physical Chemistry A, 2009. **113**(1): p. 305-314.

39. Choi, C.H. and M. Kertesz, *Conformational Information from Vibrational Spectra of Styrene, trans-Stilbene, and cis-Stilbene.* The Journal of Physical Chemistry A, 1997. **101**(20): p. 3823-3831.

40. Dae-won Chung and T. Kim, *Solvent effect on the hydrosilation reactions for the synthesis of polydimethyl siloxane grafted polyoxyethylene catalyst by Speier's catalyst.* Journal of Industrial and Engineering Chemistry, 2008. **13**(6): p. 979-84.

41. Saxena, K., C.S. Bisaria, and A.K. Saxena, *Studies on the synthesis and thermal properties of alkoxysilane-terminated organosilicone dendrimers.* Applied Organometallic Chemistry, 2010. **24**(3): p. 251-256.

42. Safa, K.D., et al., *Trisyl modification of epoxy- and chloromethyl-polysiloxanes.* Journal of the Iranian Chemical Society, 2008. **5**(1): p. 37-47.

43. Hou, S.-S., et al., *Function and performance of silicone copolymer. Part IV. Curing behavior and characterization of epoxy–siloxane copolymers blended with diglycidyl ether of bisphenol-A.* Polymer, 2000. **41**(9): p. 3263-3272.

44. Evans, J., C.A. Vincent, and P.G. Bruce, *Electrochemical measurement of transference numbers in polymer electrolytes.* Polymer, 1987. **28**(13): p. 2324-2328.

45. Renner, H., et al., *Platinum Group Metals and Compounds*, in *Ullmann's Encyclopedia of Industrial Chemistry*. 2000, Wiley-VCH Verlag GmbH & Co. KGaA.

46. Rutnakornpituk, M., P. Ngamdee, and P. Phinyocheep, *Preparation and properties of polydimethylsiloxane-modified chitosan.* Carbohydrate Polymers, 2006. **63**(2): p. 229-237.

47. Wilson, J., G. Ravi, and M.A. Kulandainathan, *Electrochemical studies on inert filler incorporated poly (vinylidene fluoride - hexafluoropropylene) (PVDF - HFP) composite electrolytes.* Polímeros, 2006. **16**: p. 88-93.

48. Shalu, et al., *Thermal Stability, Complexing Behavior, and Ionic Transport of Polymeric Gel Membranes Based on Polymer PVdF-HFP and Ionic Liquid, [BMIM][BF4].* The Journal of Physical Chemistry B, 2013. **117**(3): p. 897-906.

49. Sun, Y., et al., *A Polyamide Single-Ion Electrolyte Membrane for Application in Lithium-Ion Batteries.* Energy Technology, 2014. **2**(8): p. 698-704.

50. Rohan, R., et al., *Functionalized polystyrene based single ion conducting gel polymer electrolyte for lithium batteries.* Solid State Ionics, 2014. **268 B**: p. 294-299.

51. Malmonge, L.F., J.A. Malmonge, and W.K. Sakamoto, *Study of pyroelectric activity of PZT/PVDF-HFP composite.* Materials Research, 2003. **6**: p. 469-473.

52. Sun, X.-G. and J.B. Kerr, *Synthesis and Characterization of Network Single Ion Conductors Based on Comb-Branched Polyepoxide Ethers and Lithium Bis(allylmalonato)borate.* Macromolecules, 2005. **39**(1): p. 362-372.

53. Wang, X., et al., *A single-ion gel polymer electrolyte based on polymeric lithium tartaric acid borate and its superior battery performance.* Solid State Ionics. **262**(0): p. 747-753.

54. Jiang, J., et al., *Gel polymer electrolytes prepared by in situ polymerization of vinyl monomers in room-temperature ionic liquids.* Reactive and Functional Polymers, 2006. **66**(10): p. 1141-1148.

55. Voice, A.M., et al., *Thermo reversible gel polymer electrolyte.* Polymer, 1994. **35**(16): p. 3363.

56. Ghosh, A., C. Wang, and P. Kofinas, *Block Copolymer Solid Battery Electrolyte with High Li-Ion Transference Number.* Journal of The Electrochemical Society, 2010. **157**(7): p. A846-A849.

57. Idris, N.H., et al., *Microporous gel polymer electrolytes for lithium rechargeable battery application.* Journal of Power Sources, 2012. **201**(0): p. 294-300.

58. Xiao, J., et al., *Hybrid Air-Electrode for Li/Air Batteries.* Journal of The Electrochemical Society, 2010. **157**(3): p. A294-A297.

59. Doyle, M., T.F. Fuller, and J. Newman, *The importance of the lithium ion transference number in lithium/polymer cells.* Electrochimica Acta, 1994. **39**(13): p. 2073-2081.